STATISTICAL MODELING OF FATIGUE CRACK GROWTH RATE IN INCONEL ALLOY 600 AND 7475-T7351 ALUMINUM ALLOY

Kassim S. Al-Rubaie
EMBRAER (Empresa Brasileira de Aeronáutica), Av. Brigadeiro Faria Lima 2170
12227-901 São José dos Campos - SP, Brazil
kassim.rubaie@embraer.com.br

Leonardo B. Godefroid
Universidade Federal de Ouro Preto, Escola de Minas, Dept. de Engenharia
Metalúrgica e de Materiais, Praça Tiradentes 20, 35400-000 Ouro Preto - MG, Brazil
leonardo@demet.em.ufop.br

Emerson K.L. Barroso
CVRD (Companhia Vale do Rio Doce), Av. Dante Michelini 5500, 29090-900 Vitória - ES, Brazil
emerson.barroso@cvrd.com.br

Jadir A.M. Lopes
Centro de Desenvolvimento da Tecnologia Nuclear - CDTN/CNEN, Cidade Universitária
Pampulha, 30123-970 Belo Horizonte - MG, Brazil
jaml@cdtn.br

Abstract. *In this study, fatigue crack growth rate (FGCR) of an Inconel alloy 600 and a 7475-T7351 aluminum alloy were evaluated in air and at room temperature under constant amplitude loading at stress ratios of 0.1 and 0.5, using compact tension C(T) specimens. Three FCGR models, namely, Collipriest, Priddle, and NASGRO were examined. To handle the effect of stress ratio on FCGR, Walker equivalent stress intensity factor model was used. Consequently, generalized Collipriest (GC), generalized Priddle (GP), and generalized NASGRO (GN) models were developed and fitted to the FCGR data. It was shown that both GC and GP models fit the FCGR data in a similar fashion. However, the GP model provided a better fit than the GC model. The GN model was found to be the most appropriate model for the data. Therefore, this model may be suggested for use in critical applications, such as aeronautical structural design.*

Keywords: *Statistical modeling, Fatigue crack growth rate, Inconel alloy 600, 7475-T7351 alloy.*

1. INTRODUCTION

The determination of the safe-life of an engineering component exposed to cyclic loading conditions should be based on a detailed knowledge of the entire continuum of damage mechanisms (Bolotin, 1999). Hence, a quantitative knowledge of both fatigue and fatigue crack growth processes is necessary for safety and reliability estimation (Ellyin, 1997).

Due to the complexity of fatigue process and therefore to the lack of an accurate physical model, even today most of our basic knowledge on fatigue behavior comes from experiments. Because of the inherent randomness in fatigue data, the information contained in the data may be represented via statistical modeling.

Since the growth of macro cracks takes a significant part of the fatigue life of a structure, it is very important to predict the life of the structure after the crack has initiated. Moreover, there are many situations where macro cracks are assumed to be present in a structure and tolerated during the service life. Therefore, the methods used to predict fatigue crack growth rate (FCGR) are of essential practical interest.

Inconel alloy 600 is widely employed in a variety of applications. For its strength and corrosion resistance (Crum, 1992), it is used extensively in the chemical industry. Due to its strength and oxidation resistance at high temperatures, it is used for many applications in the heat-treating industry. In the aeronautical field, this alloy is used for a variety of engine and airframe components that must withstand high temperatures. In nuclear engineering, tubes of a pressurized water reactor (PWR) steam generator are generally made of Inconel alloys 600 and 690.

7475 (Al-Zn-Mg-Cu) aluminum alloy (Cieslak and Mehr, 1985) is widely used in aircraft industries due to high strength coupled with good fracture toughness and stress corrosion cracking resistance. This alloy is basically a modified version of 7075 aluminum alloy. Properties of 7075 are modified by a considerable reduction in the levels of iron, silicon, and manganese, but also from improvements in thermo-mechanical and heat treatment practices. These modifications result in the development of 7475 alloy.

In this work, due to a variety of applications of Inconel 600 and 7475-T7351 alloys, four FCGR data sets were collected from these alloys. One data set was collected from Inconel alloy 600 at a stress ratio *(R)* of 0.1. The other data sets were collected from 7475-T7351 aluminum alloy at *R* ratios of 0.1 and 0.5. In some cases, 7475-T7351 is being used after application of certain levels of pre-strain. Regarding the influence of pre-straining on FCGR, few works (Schijve, 1976; Nian and Bai-Ping, 1992) have been published. Therefore, two data sets were collected under conditions for pre-straining levels of 3% and 5%. As a baseline, the 0% pre-straining condition was considered.

Due to the sigmoidal shape of FCGR curve, Collipriest (Collipriest, 1972), Priddle (Anderson, 1995), and NASGRO (Forman and Mettu, 1992) models were chosen to model the data of Inconel alloy 600. To handle the effect of *R* ratio on FCGR in 7475-T7351 alloy, Walker equivalent stress intensity factor model (Walker, 1970) was used. Consequently, generalized Collipriest (GC), generalized Priddle (GP), and generalized NASGRO (GN) models were developed and fitted to the 7475-T7351 data.

2. MATERIAL AND EXPERIMENTAL PROCEDURE

The chemical composition of Inconel alloy 600 and 7475-T7351 are shown in Tables. 1 and 2.

Table 1. Chemical composition of Inconel alloy 600 (wt.%).

C	S	Fe	Cr	Ni
0.070	0.0007	9.46	13.92	70.12

Table 2. Chemical composition of the 7475 aluminum alloy (wt.%).

Alloy	Si	Fe	Cu	Mn	Mg	Zn	Cr	Ti	Al
7475	0.029	0.085	1.661	0.01	2.376	5.722	0.21	0.0266	Balance

The C(T) specimens used for fracture toughness and for fatigue crack growth tests were machined in L-T direction, according to ASTM E647 (2001); the specimen dimensions are shown in Figure 1.

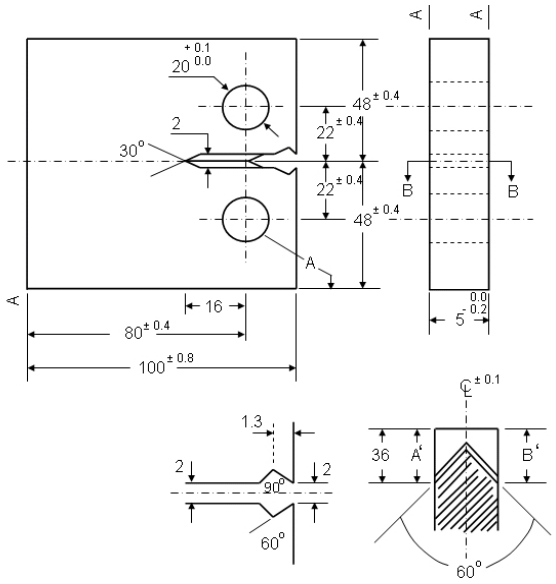

Figure 1. Dimensional details of the C(T) specimen (dimensions in mm).

Fatigue crack growth tests were conducted on pre-cracked C(T) specimens according to ASTM E 647. These tests were done in air and at room temperature under constant amplitude loading with *R* ratios of 0.1 and 0.5. The crack length was measured using a compliance method. Moreover, fatigue crack growth threshold *(ΔK_{th})* was evaluated using a constant *R* load reduction "load shedding" method proposed in ASTM E647. The ΔK_{th} is about the ΔK corresponding to a FCGR *(da/dN)* of 10^{-10} m/cycle. Fracture toughness tests were conducted on the C(T) specimens at room temperature and in air environment, according to ASTM E561 (2001). Basically, cyclic loading is applied to introduce a fatigue crack. When the crack reaches the desired length, the fatigue cycling is stopped and the load is gradually increased until fracture occurs. The stress intensity at instability was calculated as the fracture toughness K_c.

3. RESULTS AND DISCUSSIONS

3.1. Mechanical behavior

The results of the mechanical properties of Inconel alloy 600 are presented in Table 3.

Table 3. Room temperature mechanical properties of Inconel alloy 600.

σ_{YS}, MPa	σ_{UTS}, MPa	ε, %	Hardness,	K_c, MPa√m	$\Delta K_{th,}$ MPa√m
386	687	33.5	224	40.08	6.38

The results of the mechanical properties of 7475-T7351 aluminum alloy are presented in Table 4. Both 0.2% yield and ultimate tensile strength increase with an increase in the pre-strain level from 0 to 5%. On the other hand, the total strain to fracture decreases. The fracture toughness decreases with an increase in the pre-strain level. A pre-straining of 5% causes a reduction of 17% in K_c. These results are expected due to the effect of strain-hardening that leads to an increase in material strength (Liaw and Landes, 1988).

Table 4. Room temperature mechanical properties of 7475-T7351.

Pre-strain	σ_{YS}, MPa	σ_{UTS}, Mpa	ε, %	K_c, MPa√m
0%	405.76	482.60	12.11	95.5
3%	412.17	496.38	9.82	92.8
5%	416	497.67	8.82	79.3

σ_{YS}: 0.2% yield tensile strength, σ_{UTS}: ultimate tensile strength, ε: total strain.

Table 5 shows the results of the threshold stress intensity factor range *(ΔK_{th})* tests of 7475-T7351 for all cases of pre-strain studied. At the same pre-strain condition, ΔK_{th} decreases with increasing the R ratio. For 0% pre-strain, a reduction of 28% in ΔK_{th} is observed with increasing the R ratio from 0.1 to 0.5. At R = 0.1, ΔK_{th} decreases with an increase in pre-strain level; a pre-straining of 5% causes a reduction of 19% in ΔK_{th}. However, at R = 0.5, a clear relation was not found. A detailed discussion about the effects of R ratio and pre-strain on the fatigue threshold was given in (Al-Rubaie et al., 2007).

Table 5. Fatigue threshold values of 7475-T7351.

Pre-strain level	ΔK_{th}, MPa√m	
	R = 0.1	R = 0.5
0%	1.81	1.31
3%	1.65	1.45
5%	1.46	1.37

3.2. FCGR models

The reason for building models is to link theoretical ideas with the observed data to provide a good prediction of future observations. Modeling of FCGR data has enhanced the ability to create damage tolerant design philosophies.

Due to the sigmoidal shape of FCGR curve, three models that fit all parts of FCGR curve are considered. These are:

1. Collipriest model (Collipriest, 1972)

$$\frac{da}{dN} = C\left(K_c\ \Delta K_{th}\right)^{\frac{n}{2}} \exp\left[\ln\left(\frac{K_c}{\Delta K_{th}}\right)^{\frac{n}{2}} \tanh^{-1}\frac{\ln\left(\dfrac{\Delta K^2}{\Delta K_{th}\ K_c\left(1-R\right)}\right)}{\ln\left(\dfrac{K_c\left(1-R\right)}{\Delta K_{th}}\right)}\right] \tag{1}$$

2. Priddle model (Anderson, 1995)

$$\frac{da}{dN} = C\left(\frac{\Delta K - \Delta K_{th}}{K_c - \dfrac{\Delta K}{(1-R)}}\right)^n \tag{2}$$

3. NASGRO model (Forman and Mettu, 1992)

$$\frac{da}{dN} = \frac{C\,\Delta K^{n}\left(1-\frac{\Delta K_{th}}{\Delta K}\right)^{p}}{\left(1-\frac{\Delta K}{K_c(1-R)}\right)^{q}} \tag{3}$$

Equations (1-3) may be used only to fit one FCGR data set for a given R ratio. If the data at hand are collected at $R = 0.1$, the fitting models (1-3) can not be used to estimate FCGR at another R, for example, at $R = 0.5$.

To handle the effect of R on FCGR, Walker (Walker, 1970) proposed the equivalent stress intensity factor model, which is widely accepted. It is given by:

$$\Delta K_{eq} = K_{\max}\,(1-R)^{m} \tag{4}$$

m is a Walker exponent and its objective is to control the spread of the FCGR curves for different values of R; ΔK_{eq} is an equivalent zero-to-tension ($R = 0$) stress intensity factor range. Knowing that $\Delta K = K_{max}\,(1 - R)$, then:

$$\Delta K_{eq} = \Delta K\,(1-R)^{m-1} \tag{5}$$

In Equations (1-3), substituting ΔK with ΔK_{eq}, putting $R = 0$, and replacing ΔK_{th} by K_0, the generalized Collipriest (GC), generalized Priddle (GP), and generalized NASGRO (GN) models respectively may be written as:

$$\frac{da}{dN} = C\,(K_c\;K_0)^{\frac{n}{2}}\,\exp\left[\ln\left(\frac{K_c}{K_0}\right)^{\frac{n}{2}}\,\tanh^{-1}\frac{\ln\left(\frac{\Delta K^{2}\,(1-R)^{2m-2}}{K_0\;K_c}\right)}{\ln\left(\frac{K_c}{K_0}\right)}\right] \tag{6}$$

$$\frac{da}{dN} = C\left(\frac{\Delta K\,(1-R)^{m-1}-K_0}{K_c-\Delta K\,(1-R)^{m-1}}\right)^{n} \tag{7}$$

$$\frac{da}{dN} = \frac{C\left(\Delta K\,(1-R)^{m-1}\right)^{n}\left(1-\frac{K_0}{\Delta K\,(1-R)^{m-1}}\right)^{p}}{\left(1-\frac{\Delta K\,(1-R)^{m-1}}{K_c}\right)^{q}} \tag{8}$$

where C, n, m, p, q are model parameters estimated from experimental data and K_0 is the threshold value at $R = 0$.

The influence of R on ΔK_{th} can be described by Klesnil and Lukáš equation (Klesnil and Lukáš, 1992):

$$\Delta K_{th,R} = \Delta K_{th,0}\,(1-R)^{\gamma} \tag{9}$$

where $\Delta K_{th,R}$ is the threshold stress intensity factor range for a given R, $\Delta K_{th,0}$ is the threshold value for $R = 0$, which equals K_0, and γ is the fitting parameter lying between 0 and 1.

In Equations (6-8), R is an independent variable; it implies that FCGR data sets collected at different R ratios can be joined for the statistical analysis. Hence, the generalized fitting models (6-8) may be used to interpolate FCGR for R ratios that were not considered in the testing program, thereby reducing both time and cost.

3.3. Model fitting

Equations (1-3) and (6-8) are nonlinear regression models. A nonlinear model has at least one parameter that appears nonlinearly (Bates and Watts, 1988). Nonlinear regression is an iterative procedure, and the basis used for estimating the unknown parameters is the criterion of least-squares.

The least-squares criterion quantifies goodness of fit as the sum of squares of the vertical distances of the data points from the assumed model. That is, the best model for a particular data set is that with the smallest sum of squares. In fact, it is not simple to compare models with different parameters. The problem is that a more complicated model (more parameters) gives more inflection points for the curve being generated than the curve being defined by a simpler model (fewer parameters). Thereby, the sum of squares of a more complicated model tends to be lower.

A. Inconel alloy 600

Equations (1-3) were used for the nonlinear regression analysis. Collipriest [Equation (1)] and Priddle [Equation (2)] models use two parameters *(C, n)*, while the NASGRO [Equation (3)] contains four parameters *(C, n, p, q).* The objective of p and q is to provide a better fit to data in near-threshold and accelerated regions, respectively. The parameters p and q may

be fixed, reducing the model parameters to two. For metallic materials, since the values of p and q are between 0 and 1, they were chosen by trial end error to be 0.30 and 0.70, respectively.

A visual examination of the fitting curves in Figure 2 reveals that both Collipriest and Priddle models fit the FCGR data in a similar fashion. The NASGRO model offers the best approximation of the data.

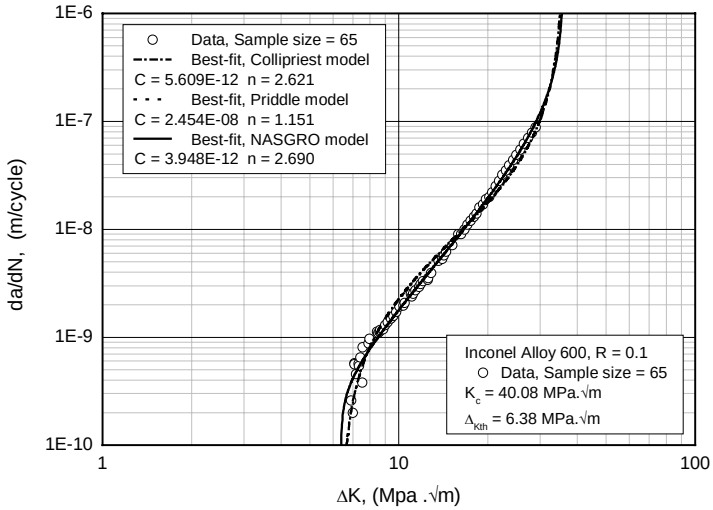

Figure 2. FCGR comparative curves of Inconel alloy 600, R = 0.1.

The estimated parameters and the statistical properties for FCGR models are presented in Table. 6. From Table 6a, at the 0.05 level of significance, it may be concluded that the estimated parameters *(C, n)* are statistically significant, since their *p-values* are smaller than the level of significance. From Table 6b, it can be seen that all statistical properties of NASGRO model are better than the other two models. Therefore, NASGRO model may be considered the most appropriate model that approximates the real process given the data.

Table 6a. Estimated parameters of FCGR models, Inconel alloy 600, R = 0.1.

Model	Parameter	Estimate	Std. error	t –value	p-value	95% LCL	95% UCL
Collipriest	C	5.609E–12	7.023E–13	7.987	< 0.0001	4.206E–12	7.012E–12
	n	2.621	4.809E–02	54.508	< 0.0001	2.525	2.718
Priddle	C	2.454E–08	1.015E–09	24.176	< 0.0001	2.252E–08	2.657E–08
	n	1.151	2.034E–02	56.60	< 0.0001	1.111	1.192
NASGRO	C	3.948E–12	4.310E–13	9.159	< 0.0001	3.086E–12	4.809E–12
	n	2.690	4.205E–02	63.962	< 0.0001	2.606	2.774

Table 6b. Statistical properties of FCGR models, Inconel alloy 600, R = 0.1.

Model	SSE	SE	MSE	R^2	R^2_{adj}
Collipriest	0.63614	0.10049	0.01010	0.9792	0.9789
Priddle	0.59086	0.09684	0.00938	0.9807	0.9804
NASGRO	0.25591	0.06373	0.00406	0.9917	0.9915

SSE: sum of squares of error, SE: standard error of the residual, MSE: mean squared error
R^2: coefficient of determination, R^2_{adj}: adjusted coefficient of determination
LCL: lower confidence limit, UCL: upper confidence limit.

B. 7475-T7351 aluminum alloy

Equations (6-8) were used for the nonlinear regression analysis. Both GC [Equation (6)], and GP [Equation (7)] models use three parameters *(C, n, m)*, while the GN model [Equation (8)] contains five parameters *(C, n, m, p, q).* Hence, the parameters p and q may be fixed and were chosen by trial end error to be 0.20 and 0.80, respectively.

The experimental data and the estimated curves are shown in Figure 3. For the cases of 0%, 3%, and 5% pre-strain, a visual examination of the fitting curves reveals that the GC and GP models fit the FCGR data in a similar fashion; however, the latter fits relatively better than the former. The GN model offers the best approximation of the data.

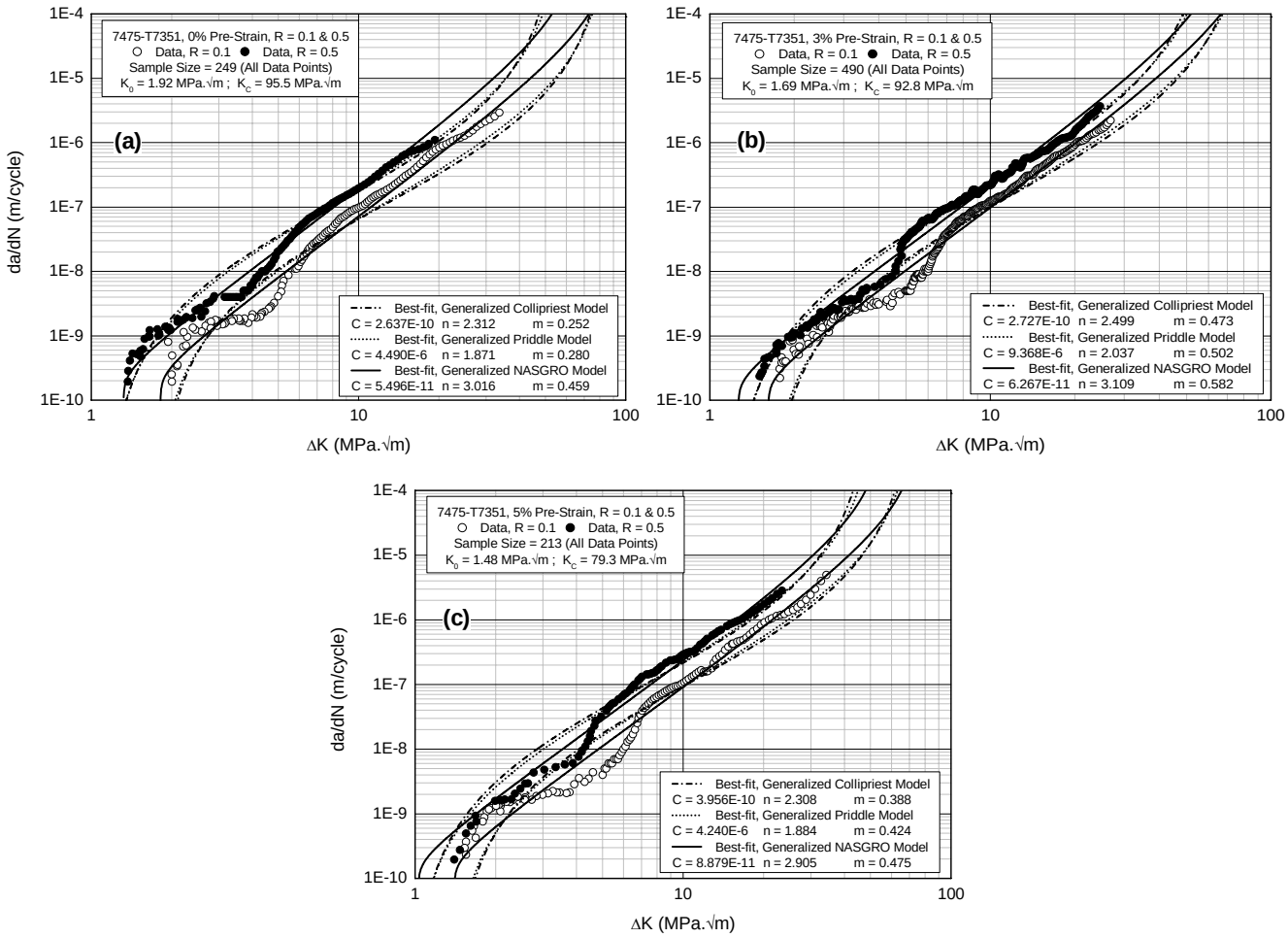

Figure 3. FCGR comparative curves of 7475-T7351: (a) 0% pre-strain, (b) 3% pre-strain, and (c) 5% pre-strain.

From Tables 7a-9a, at the 0.05 level of significance, it may be concluded that the estimated parameters *(C, n, m)* are statistically significant, since their *p-values* are smaller than the level of significance. Tables 7b-9b show that the statistical properties of the GP model are better than these of the GC model. In addition, the GN model gives the best statistical properties. Therefore, the GN model seems to be the best approximating model to the data.

Table 7a. Estimated parameters of FCGR models, 7475-T7351, 0% pre-strain.

Model	Parameter	Estimate	Std. error	t-value	p-value	95% LCL	95% UCL
Generalized Collipriest (GC)	C	2.637E−10	3.648E−11	7.227	< 0.0001	1.918E−10	3.355E−10
	n	2.312	5.272E−02	43.861	< 0.0001	2.208	2.416
	m	0.252	3.544E−02	7.097	< 0.0001	0.182	0.321
Generalized Priddle (GP)	C	4.490E−06	4.647E−07	9.663	< 0.0001	3.575E−06	5.406E−06
	n	1.871	3.679E−02	50.849	< 0.0001	1.798	1.943
	m	0.280	3.212E−02	8.721	< 0.0001	0.217	0.343
Generalized NASGRO (GN)	C	5.496E−11	4.132E−12	13.300	< 0.0001	4.682E−11	6.310E−11
	n	3.016	3.076E−02	98.066	< 0.0001	2.956	3.077
	m	0.459	2.145E−02	21.410	< 0.0001	0.417	0.501

Table 7b. Statistical properties of FCGR models, 7475-T7351, 0% pre-strain.

Model	SSE	SE	MSE	F	R^2	R^2_{adj}
Generalized Collipriest (GC)	25.0316	0.3189	0.1018	1253.9	0.9107	0.9099
General Priddle (GP)	19.7155	0.2831	0.0801	1625.2	0.9296	0.9291
General NASGRO (GN)	5.8494	0.1542	0.0238	5769.4	0.9791	0.9790

Table 8a. Estimated parameters of FCGR models, 7475-T7351, 3% pre-strain.

Model	Parameter	Estimate	Std. error	t-value	p-value	95% LCL	95% UCL
Generalized Collipriest (GC)	C	2.727E−10	2.147E−11	12.704	< 0.0001	2.306E−10	3.149E−10
	n	2.499	2.908E−02	85.966	< 0.0001	2.443	2.557
	m	0.473	2.276E−02	20.772	< 0.0001	0.428	0.517
Generalized Priddle (GP)	C	9.368E−06	5.276E−07	17.755	< 0.0001	8.331E−06	1.040E−05
	n	2.037	2.004E−02	101.588	< 0.0001	1.997	2.076
	m	0.502	2.001E−02	25.086	< 0.0001	0.463	0.541
Generalized NASGRO (GN)	C	6.267E−11	2.951E−12	21.238	< 0.0001	5.687E−11	6.847E−11
	n	3.109	1.995E−02	155.914	< 0.0001	3.071	3.149
	m	0.582	1.423E−02	40.933	< 0.0001	0.554	0.611

Table 8b. Statistical properties of FCGR models, 7475-T7351, 3% pre-strain.

Model	SSE	SE	MSE	F	R^2	R^2_{adj}
Generalized Collipriest (GC)	28.7749	0.2431	0.0591	3997.9	0.9426	0.9424
General Priddle (GP)	21.4729	0.2099	0.0441	5440.3	0.9572	0.9570
General NASGRO (GN)	8.6857	0.1335	0.0178	13808	0.9827	0.9826

Table 9a. Estimated parameters of FCGR models, 7475-T7351, 5% pre-strain.

Model	Parameter	Estimate	Std. error	t-value	p-value	95% LCL	95% UCL
Generalized Collipriest (GC)	C	3.956E−10	5.173E−11	7.647	< 0.0001	2.936E-10	4.976E-10
	n	2.308	4.761E−02	48.467	< 0.0001	2.214	2.402
	m	0.388	5.601E−02	6.936	< 0.0001	0.278	0.499
Generalized Priddle (GP)	C	4.240E−06	4.407E−07	9.621	< 0.0001	3.371E−06	5.109E−06
	n	1.884	3.393E−02	55.538	< 0.0001	1.817	1.951
	m	0.424	4.953E−02	8.565	< 0.0001	0.327	0.522
Generalized NASGRO (GN)	C	8.879E−11	7.049E−12	12.597	< 0.0001	7.490E−11	1.027E−10
	n	2.905	3.437E−02	84.528	< 0.0001	2.837	2.973
	m	0.475	3.051E−02	15.557	< 0.0001	0.415	0.535

Table 9b. Statistical properties of FCGR models, 7475-T7351, 5% pre-strain.

Model	SSE	SE	MSE	F	R^2	R^2_{adj}
Generalized Collipriest (GC)	20.9811	0.3161	0.0999	1196.1	0.9193	0.9185
General Priddle (GP)	16.4431	0.2798	0.0783	1555.2	0.9367	0.9362
General NASGRO (GN)	6.2933	0.1731	0.0299	4232.7	0.9758	0.9756

3.4. Model validation

There are many graphical and numerical tools to assist goodness of fit of a model used with experimental data (Chambers et al., 1983; Devore and Farnum, 1999). The most common approach is to examine the residual.

A. Inconel alloy 600

The histogram plots presented in Figure 4 suggest that the residuals (measured - predicted) of the NASGRO model appear to be approximate the normal distribution when some extreme points were removed. This indicates that the NASGRO model is better than the other model.

Figure 4d illustrates the box plots of residual data of FCGR models. The variability in the residual data obtained from Collipriest and Priddle models appears to be similar. The NASGRO model gives less variability. In addition, outliers (extreme values) as indicated by the (o) symbols were detected. Due to the small range of the whiskers and length of the box, it may be concluded that the NASGRO model is the most approximating model to the data.

To assess the model goodness of fit, several statistical numerical measures may be checked such as R^2, R^2_{adj}, *F*, *SE*, *MSE,* Schwarz's Bayesian Information Criterion *(BIC)*, and Akaike's Information Criterion *(AIC)* (Burnham and Anderson, 2002; Al-Rubaie et al., 2007a). Large value of *F*, small values of *SE and MSE* indicate that the model explains the data well. Table 6b suggests that the NASGRO model provides a better fit than the other models used.

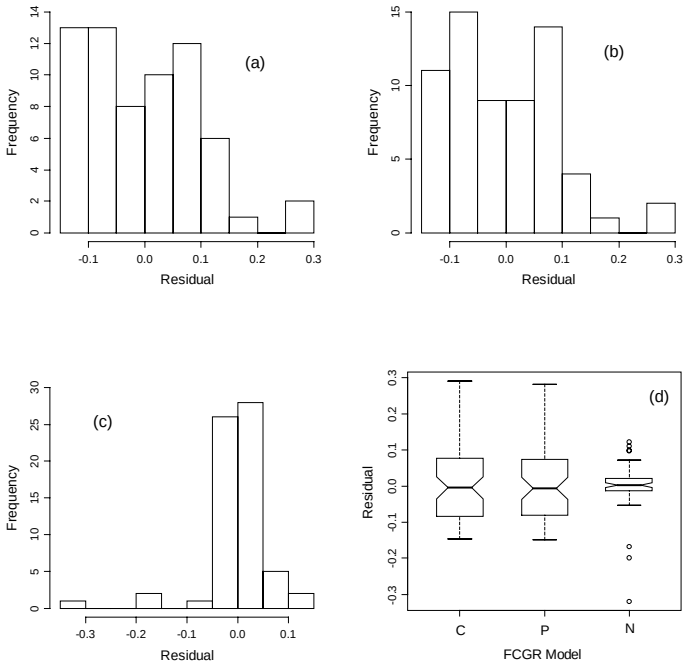

Figure 4. Residual data of FCGR models, Inconel alloy 600, R = 0.1: (a) Collipriest model (C), (b) Priddle model (P), (c) NASGRO (N) model, and (d) Box plot.

B. 7475-T7351 aluminum alloy

The histogram plots presented in Figures 5-7 suggest that the residuals of the GN model appear to be normally distributed. This desirable result indicates that the GN model is satisfactory.

Figures 5d-7d illustrate box plots of the residual data of the FCGR models. The variability in the residual data obtained from the GC model appears much greater than that from the GP model. In addition, outliers were detected. Due to the small range of the whiskers and length of the box, it may be concluded that the GN model is the most approximating model to the data.

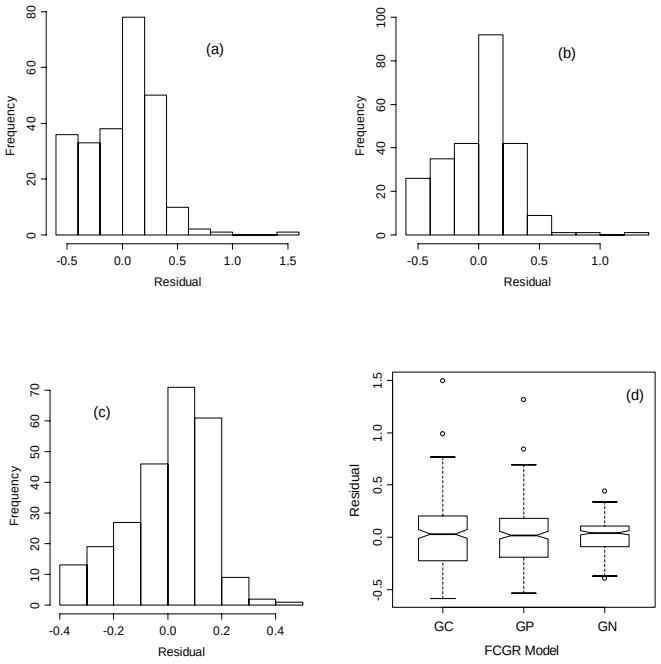

Figure 5. Residual data of FCGR models, 7475-T7351, 0% pre-strain: (a) Generalized Collipriest model (GC), (b) Generalized Priddle model (GP), (c) Generalized NASGRO model (GN), and (d) Box plot.

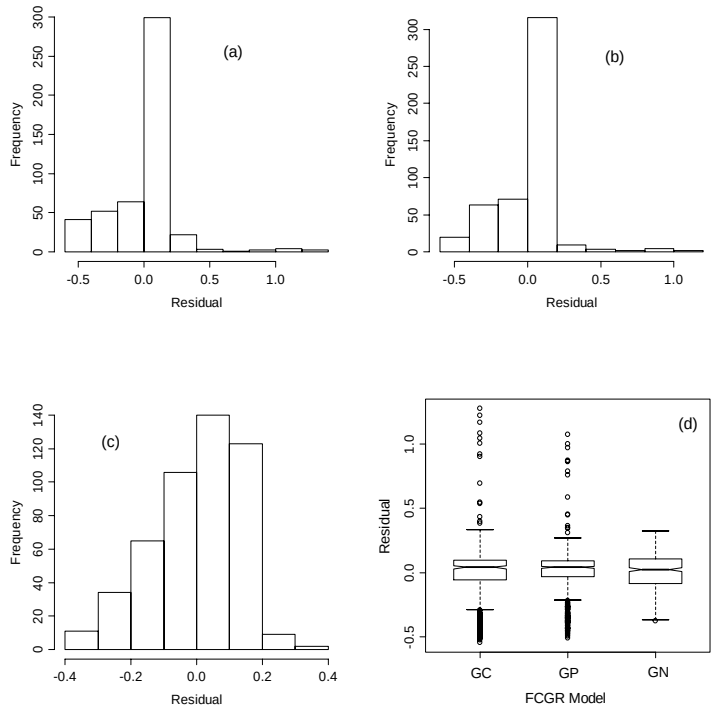

Figure 6. Residual data of FCGR models, 7475-T7351, 3% pre-strain: (a) Generalized Collipriest model (GC), (b) Generalized Priddle model (GP), (c) Generalized NASGRO model (GN), and (d) Box plot.

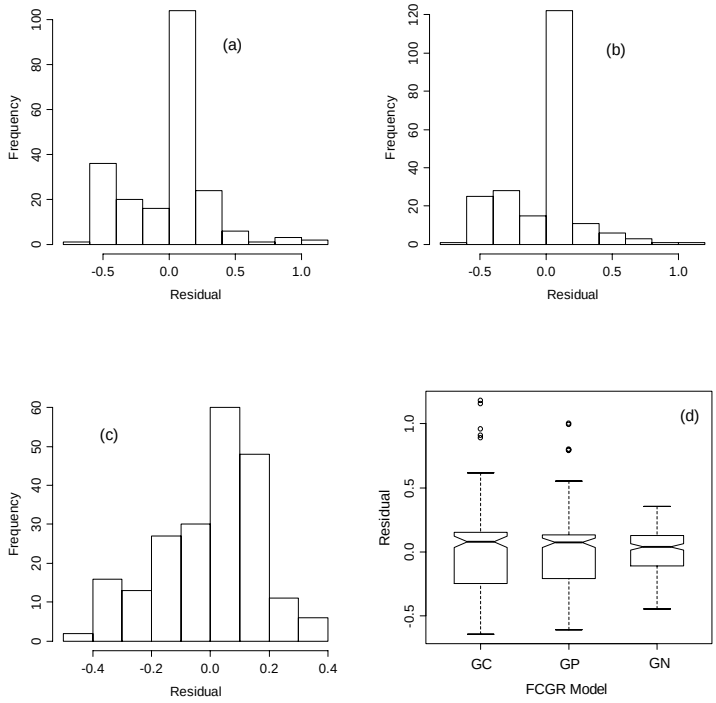

Figure 7. Residual data of FCGR models, 7475-T7351, 5% pre-strain: (a) Generalized Collipriest model (GC), (b) Generalized Priddle model (GP), (c) Generalized NASGRO model (GN), and (d) Box plot.

4. CONCLUSIONS

Fatigue crack growth rate (FCGR) in Inconel alloy 600 and in pre-strained 7475-T7351 aluminum alloy were evaluated in air and at room temperature under constant amplitude loading at stress ratios of 0.1 and 0.5, using compact tension specimens. Due to the sigmoidal shape of FCGR curve, Collipriest, Priddle, and NASGRO models were chosen to model the data of Inconel alloy 600. To handle the effect of stress ratio *(R)* on FCGR in 7475-T7351 alloy, Walker model was used. Consequently, generalized Collipriest (GC), generalized Priddle (GP), and generalized NASGRO (GN) models were developed and fitted to the 7475-T7351 data. For model validation, different commonly used graphical plots and statistical numerical measures were presented. From the results obtained, the following conclusions can be drawn:

1. Both Collipriest and Priddle models fit the data of Inconel alloy 600 in a similar fashion. The NASGRO model seems to be the most appropriate model to the observed data.
2. The generalized fitting models can be used to interpolate FCGR for *R* ratios that were not considered in the testing program, thereby reducing both time and cost.
3. Both generalized Collipriest and generalized Priddle models fit the FCGR data of pre-strained 7475-T7351 in a similar fashion. However, the latter provides a better fit than the former. The generalized NASGRO (GN) model is the most approximating model to the data. Therefore, this model may be suggested for use in critical applications, such as aeronautical structural design.

5. REFERENCES

Al-Rubaie, K.S., Barroso, E.K.L, Godefroid, L.B., 2007, "Statistical Modeling of Fatigue Crack Growth Rate in Pre-Strained 7475-T7351 Aluminum Alloy", Submitted to Materials Science and Engineering A.

Al-Rubaie, K.S., Godefroid, L.B., Lopes, J.A.M., 2007a, "Statistical Modeling of Fatigue Crack Growth Rate in Inconel Alloy 600", International Journal of Fatigue, Vol. 29, pp. 931-940.

Anderson, T.L., 1995, "Fracture Mechanics: Fundamentals and Applications", CRC Press, Second Ed., 688 p.

ASTM E561, 2001, "Standard Practice for R-Curve Determination", Annual Book of ASTM Satandards, ASTM.

ASTM E647, 2001, "Standard Test Method for Measurement of Fatigue Crack Growth Rates", Annual Book of ASTM Standards, ASTM.

Bates, D.M., Watts, D.G., 1988, "Nonlinear Regression Analysis and its Applications", John Wiley & Sons, 365 p.

Bolotin, V.V., 1999, "Mechanics of Fatigue", CRC Press, 463 p.

Burnham, K.P., Anderson, D.R., 2002, "Model Selection and Multimodel Inference: A Practical Information-Theoretic Approach", Springer, Second Ed., 496 p.

Chambers, J.M., Cleveland, W.S., Kleiner, B., Tukey, P.A., 1983, "Graphical Methods for Data Analysis", Duxbury Press, 395 p.

Cieslak, S.J., Mehr, P.L., 1985, "Alcoa 7475 Sheet and Plate", Alcoa Green Letter, Fourth Revised Ed., 47 p.

Collipriest, J.E., 1972, "An Experimentalist's View of the Surface Flaw Problem", ASME, pp. 43-61.

Crum, J.R., 1992, "Major Applications and Corrosion Performance of Nickel Alloys", in: Corrosion, ASM Handbook, Vol. 13, ASM, 1992.

Devore, J.L., Farnum, N.R., 1999, "Applied Statistics for Engineers and Scientists", Duxbury Press, First Ed., 577 p.

Ellyin, F., 1997, "Fatigue Damage, Crack Growth and Life Prediction", Chapman & Hall, 469 p.

Forman, R.G., Mettu, S.R., 1992, "Behavior of Surface and Corner Cracks Subjected to Tensile and Bending Loads in Ti-6Al-4V Alloy", ASTM STP 1131, pp 519-546.

Klesnil, M., Lukáš, P., 1992, "Fatigue of Metallic Materials", Elsevier Science, Second Revised Ed., 270 p.

Liaw, P.K, Landes, J.D., 1988, "Effects of Monotonic and Cyclic Prestrain on Fracture Toughness: A Summary, Fracture Mechanics", Eighteenth Symposium, ASTM STP 945, pp. 622-646.

Nian, L., Bai-Ping, D., 1992, "Effect of Monotonic and Cyclic Prestrain on the Fatigue Threshold in Medium-Carbon Steels", International Journal of Fatigue, Vol. 14, pp. 41-44.

Schijve, J., 1976, "The Effect of Pre-Strain on Fatigue Crack Growth and Crack Closure", Engineering Fracture Mechanics, Vol. 8, pp. 575-581.

Walker, E.K., 1970, "The Effect of Stress Ratio during Crack Propagation and Fatigue for 2024-T3 and 7075-T6 Aluminum: Effect of Environment and Complex Load History on Fatigue Life", ASTM STP 462, pp. 1-14.